Stability of Differentially Rotating Neutron Stars

Lukas R. Weih[1,*], Luciano Rezzolla[1,2]
*weih@th.physik.uni-frankfurt.de

[1]Institute for Theoretical Physics, Goethe University Frankfurt, Max-von-Laue Str. 1, 60438 Frankfurt am Main, Germany

[2]Frankfurt Institute for Advanced Studies, Ruth-Moufang-Str. 1, 60438 Frankfurt am Main, Germany

Introduction

The most famous result in the context of stability of relativistic stars is the turning-point criterion [1], from which follows that along a sequence of non-rotating neutron stars with constant angular momentum the models to the high-density side of the sequence's maiximum are secularly unstable, while the ones on the low-density side are stable equilibrium solutions. In Ref. [2] was found that for uniformly rotating neutron stars this criterion is just a sufficient, but not a necessary one. The onset of dynamical instability is marked by the neutral-stability line, which coincides with the turning-point for non-rotating stars and is shifted to the low-density side with increasing angular momentum.

Simulations of binary neutron star mergers have shown that the merger remnant is a differentially rotating neutron star [3]. The stability properties of such stars are still unknown. The aim of this work is therefore to find the onset of instability for differentially rotating models by dynamically evolving selected models in full GR.

Selected Models

The models to be evolved are differentially rotating neutron stars using the j-constant law

$$F(\Omega) = A^2(\Omega_c - \Omega)$$

and a polytropic EOS with $K = 100$ and $\Gamma = 2.0$. The models are chosen for a moderate degree of differential rotation $A/r_e = 5.0$ and close to their respective turning-points. Their position in the $M - \rho_c$ plain is shown in figure 1. An unstable equilibrium solution does not necessarily collapse to a black hole, but might also migrate to a stable solution depending on the direction of the truncation error. Therefore, the initial models have been perturbed by slighlty reducing their angular velocity ($\delta\Omega \sim 0.5\%$), which ensures that an unstable solution does collapse.

Numerical Setup

The initial data is constructed by the `RNSID` code [4]. This and the subsequently mentioned codes are implemented in the `Einstein Toolkit` [5]. From the initial data the necessary quantities of the $3+1$ formalism are computed and mapped onto a Cartesian grid. Fixed mesh refinement is used, which is provided by the `Carpet` driver [6]. The two refinement levels have grid resolutions of $dh_1 = 0.2M_\odot$ (~ 295m), and $dh_2 = 0.4M_\odot$ (~ 589m), respectively, with the boundary at $12M_\odot$ (~ 17.7km) and at twice that distance. In order to save computation time the neutron star's symmetry is exploited and a reflection symmetry across the $z = 0$ plane is adopted.

The spacetime is evolved by the fourth-order finite-differencing code `McLachlan` [7]. In this code the equations of the CCZ4-formulation are solved using 1+log slicing and the Gamma-driver condition for the shift. The evolution of the hydrodynamic quantities is done by the high-resolution shock-capturing `WhiskyTHC` code [8, 9] employing an ideal EOS with $\gamma = 2$. This code implements the equations of general-relativistic hydrodynamics in the conservative Valencia formulation [10] and solves them using a fourth-order finite-differencing scheme. The flux reconstruction is done by a monotonicity preserving scheme that is of fifth order in space. The time evolution of the coupled set of hydrodynamics and Einstein equations is done by the thorn `MoL` using a CFL number of 0.15.

During the simulation the `AHFinderDirect` thorn [11] detects apparent horizons and hence the formation of a black hole.

Results

In figure 1 the selected models are presented as open circles, which are red in the case of collapse and green otherwise. It is evident that the onset of dynamical instability sets in on the low-density side of the turning-point and moves further from it with increasing angular momentum. This agrees well with the known neutral-stability line for uniformly rotating neutron stars [2].

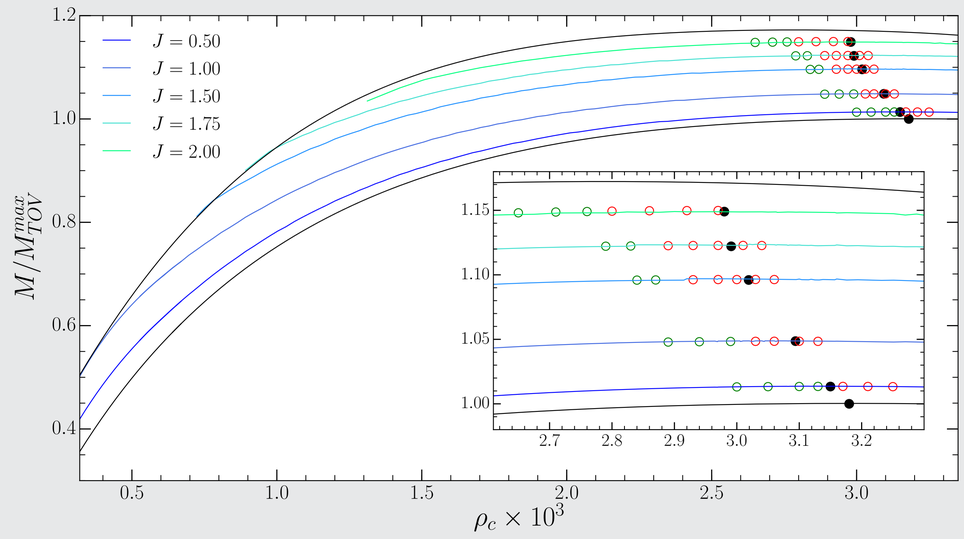

Figure 1: Equilibria of differentially rotating neutron stars. Shown is the gravitational mass M over the central rest-mass density ρ_c. The lower black line corresponds to the non-rotating models, colored lines to sequences with constant angular momentum and the upper black line to the mass-shedding limit. Also shown are the turning points (black dots) and the selected models (open circles).

Figure 2 shows the evolution of the central rest-mass density for a sequence of angular momentum $J = 1.0$. The collapse of unstable models is evident from the divergence of the rest-mass density, while for stable models it oscillates around the value of the corresponding equilibrium solution. This oscillation is induced by the initial perurbation. The picture looks qualitatively the same for all the $J = \text{const.}$ sequences.

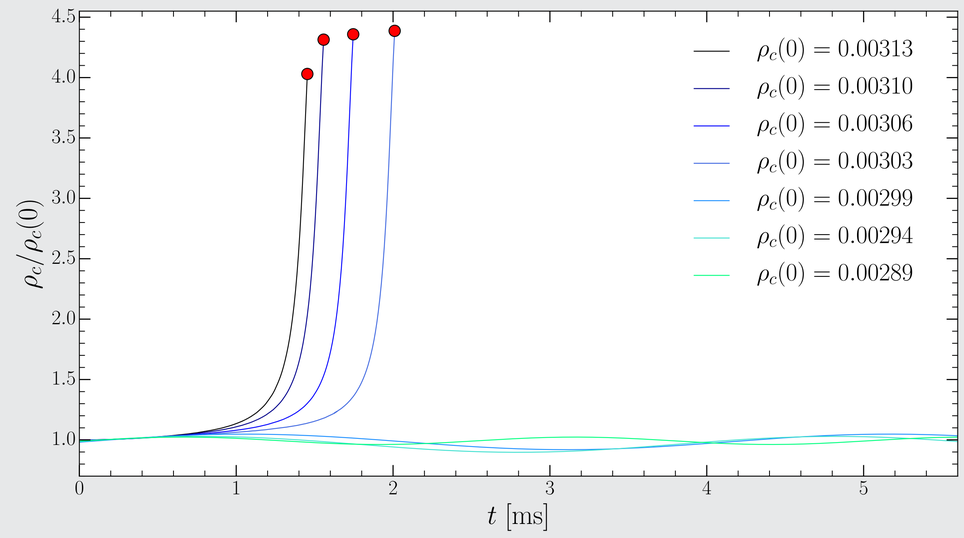

Figure 2: Time evolution of the central rest-mass density $\rho_c(t)$ normalized to its initial value $\rho_c(0)$. The lines correspond to seven models with angular momentum $J = 1.0$ and different initial values of ρ_c. For collapsing models the evolution is shown until the first detection of an apparent horizon (red dots).

Conclusion and Outlook

For the analysed models it is evident that the onset of dynamical instability sets in on the low-density side of the turning-point and moves further from it with increasing angular momentum. This agrees well with the known neutral-stability line for uniformly rotating neutron stars [2]. The equilibrium solutions are all of type A according to the classification in Ref. [12]. A similar study is yet to be done for more extreme configurations (types B, C and D). In Ref. [3], however, was shown that the differentially rotating merger remnant has a rotation profile very different to the monotonically decreasing one obtained by using the j-constant law. Hence, a stability analysis should be done for equilibrium solutions, which are constructed with a rotation law that yields a more realistic rotation profile.

References

[1] J.L. Friedmann, J.R. Ipser, and R.D. Sorkin. *Astrophys. J.*, 325:722–724, 1988.
[2] K. Takami, L. Rezzolla, and S. Yoshida. *Mon. Not. R. Astron. Soc.*, 416:L1–L5, 2001.
[3] M. Hanauske et al. arXiv:1611.07152 [gr-qc], 2016.
[4] N. Stergioulas and J.L. Friedmann. *Astrophys. J.*, 444:306–311, 1995.
[5] The Einstein Toolkit Consortium. einsteintoolkit.org.
[6] E. Schnetter, S. Hawley, and I. Hawke. *Class. Quantum Grav.*, 21:1465–1488, 2004.
[7] F. Löffler et al. *Class. Quantum Grav.*, 29:115011, 2012.
[8] D. Radice and L. Rezzolla. *Astron. Astrophys.*, 547:A26, 2012.
[9] D. Radice, L. Rezzolla, and F. Galeazzi. *Class. Quantum Grav.*, 31:075012, 2014.
[10] F. Banyuls et al. *Astrophys. J.*, 476:221–231, 1997.
[11] J. Thornburg. *Class. Quantum Grav.*, 21:743–766, 2004.
[12] L. Villain M. Ansorg, D. Gondek-Rosinska. *Mon. Not. R. Astron. Soc.*, 396:2359–2366, 2009.